



1-Butene metathesis over Mo/mordenite-alumina catalyst: Effect of sodium exchange degree in mordenite zeolite

Xiujie Li*, Dazhou Zhang, Xiangxue Zhu, Fucun Chen, Shenglin Liu, Sujuan Xie, Longya Xu*

Dalian National Laboratory for Clean Energy, Dalian Institute of Chemical Physics, Chinese Academy of Sciences, 457 Zhongshan Road, Dalian 116023, China

ARTICLE INFO

Article history:

Received 31 October 2012
Received in revised form 29 January 2013
Accepted 14 February 2013
Available online 27 February 2013

Keywords:

1-Butene
Propene
Olefin metathesis
Molybdenum
Mordenite-alumina

ABSTRACT

A series of Mo/mordenite-alumina catalysts with progressive sodium exchange degrees in mordenite were prepared and their performance in 1-butene metathesis reaction was evaluated. Significant variations in product distribution and catalytic activity were observed when the exchange degree of mordenite changed. As revealed by NH_3 -TPD and ^1H MAS NMR results, the acid site density and distribution over the catalysts were directly related to the degree of ion-exchange of sodium in mordenite. The change of support acidity led to different anchoring modes and dispersion of Mo species on the support which further resulted in the different reduction behavior of Mo species under olefin atmosphere. A good correlation between product distribution and properties of the catalysts was proposed.

© 2013 Elsevier B.V. All rights reserved.

1. Introduction

As one of the most important basic petrochemicals, nowadays the demand for propene is growing rapidly in world-wide chemical market. However, traditional processes for propene production cannot meet this growing demand. Several on-purpose propene production technologies including methanol to olefin process, steam cracking, propane dehydrogenation and catalytic cracking of C4 alkenes have been proposed [1]. In addition, olefin metathesis reaction, especially those catalyzed by supported heterogeneous catalysts, provides an alternative route to produce propene [2–4]. Compared with the cross metathesis of ethene and 2-butene to propene, 1-butene auto-metathesis has attracted more interest due to the absence of valuable ethene source [5–9]. However, due to the participation of isomerization reaction, the reaction pathway of 1-butene metathesis is more complicated as shown in Scheme 1. As propene is the target product, cross metathesis of 1-butene and 2-butene is regarded as the optimal reaction pathway for 1-butene auto-metathesis. This process requires the initial double bond isomerization of 1-butene. It is well known that acid sites could catalyze 1-butene isomerization reaction and they also participate in the following metathesis process [10–12]. Metal carbene species are the active sites for olefin metathesis. Well dispersion of metal oxide on the support will contribute to the enhancement of metathesis activity [13]. Thus, elucidating the

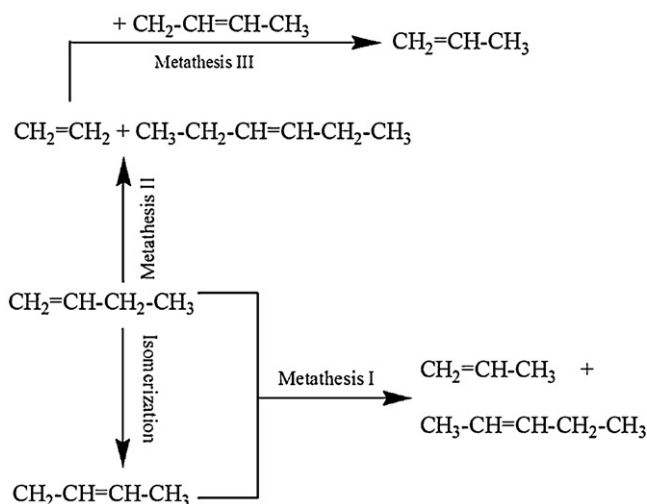
roles of catalyst acidity and its influence on metal location is of great importance for regulating the catalyst design and preparation. Our recent study showed that Mo supported on mordenite-alumina composites exhibited high activity in the 1-butene auto-metathesis reaction [8,14]. However, the function of catalyst acidity, especially the role of acid sites over mordenite zeolite on the catalyst performance should be further revealed. In this contribution, we try to elucidate the effect of sodium exchange degree of mordenite on the surface acidity, position of molybdenum within the support and redox behavior of the catalyst. A series of mordenite-alumina composites with different sodium exchange degrees were prepared and used as supports to prepare Mo/mordenite-alumina catalysts with different acidity. Quantitative acidity information before and after Mo loading was obtained from the NH_3 -TPD and ^1H MAS NMR spectra. H_2 -TPR was performed to reveal the location and redox behavior of Mo species. The results indicated that the performance of the catalysts in 1-butene auto-metathesis was well related to their acidic and redox properties.

2. Experimental

2.1. Catalyst preparation and evaluation

The mordenite-alumina composite support was prepared by extruding a mixture of $\gamma\text{-Al}_2\text{O}_3$ and NaMOR zeolite ($\text{Na}_2\text{O}\% = 6.1\%$, $\text{Si}/\text{Al} = 5.6$ provided by Fushun Petroleum Company, China) powder into extrudates with a diameter of about 2 mm. The drawn extrudates were dried at 120°C for 12 h and calcined at 540°C for 2 h. The obtained support was designed as NaM-30Al, which meant the

* Corresponding authors. Tel.: +86 411 8437 9279; fax: +86 411 8437 9279.
E-mail addresses: xiujieli@dicp.ac.cn (X. Li), lyxu@dicp.ac.cn (L. Xu).



Scheme 1. Possible metathesis reaction pathways of 1-butene.

weight percent of alumina in the support was 30%. Then, NaM-30Al was ion-exchanged with NH_4NO_3 solution at 80°C . The exchange degree can be controlled by varying the exchanging time. $\text{NH}_4\text{NaM-30Al}$ was ground into 16–32 meshes after calcination at 520°C for 2 h and denoted as $\text{H}_n\text{Na}_{100-n}\text{M-30Al}$ where n (%) stands for the exchange degree of total sodium in the support. The actual Na content was obtained by the XRF measurements. Catalysts with 6% Mo loading were prepared by wet impregnation of $\text{H}_n\text{Na}_{100-n}\text{M-30Al}$ with an aqueous solution of $(\text{NH}_4)_6\text{Mo}_7\text{O}_{24}\cdot 4\text{H}_2\text{O}$, then dried at 120°C and finally calcined at 600°C for 2 h. The catalysts were denoted as $6\text{Mo}/\text{H}_n\text{Na}_{100-n}\text{M-30Al}$, where 6 (%) stood for the weight percent of Mo atoms in the catalysts.

The catalysts (1.0 g) were tested in a fixed-bed down-flow stainless steel reactor of 7 mm in diameter with quartz sand to fix the catalyst bed. Quartz wool was applied to separate the catalyst from the quartz sand. In the middle of catalyst bed, a thermocouple was applied to detect the reaction temperature. After activation for 2 h at 550°C under nitrogen to remove the moisture, the system was cooled down to the reaction temperature at 150°C . All the reaction products were analyzed by an on-line Varian CP/3800 gas chromatograph equipped with an alumina-plot column and an FID detector. The connecting lines between the reactor outlet and the sampling valve were heated to prevent the condensation of the products with high molecular weights. 1-butene feed (1-butene 95%, butane 5%) was obtained from Dalian Special Gas Company.

The 2-butene isomers (*trans*-2-butene and *cis*-2-butene) from 1-butene isomerization are considered as feed stock. The conversion of 1-butene and selectivity are calculated using the following equations:

$$X_{\text{butene}} = \frac{[1\text{-butene}]_F - [1\text{-butene}]_P - [2\text{-butene}]_P}{[1\text{-butene}]_F} \times 100\%$$

$$S_{\text{olefin}} = \frac{[C_{\text{olefin}}]_P}{[\text{ethene}]_P + [\text{propene}]_P + [\text{pentene}]_P + [\text{hexene}]_P + [C_7^+]_P} \times 100\%$$

In the above equations, $[1\text{-butene}]_F$ represents the molar percentage of 1-butene in the feed; $[\text{ethene}]_P$, $[\text{propene}]_P$, $[2\text{-butene}]_P$, $[\text{pentene}]_P$, $[\text{hexene}]_P$, and $[C_7^+]_P$ are the molar percentage of each component in products, respectively. In addition, the heavy products having seven or more carbon atoms are denoted as C_7^+ . Carbonaceous deposits on the catalyst are not taken into account for the selectivity calculation. Y_{olefin} in the manuscript means the molar yield of the designed olefin product. And the detailed calculation method was described in Ref. [8].

2.2. Catalyst characterization

Temperature-programmed desorption of ammonia ($\text{NH}_3\text{-TPD}$) measurements were carried out in a conventional U-shaped stainless-steel micro-reactor (*i.d.* = 4 mm) using flowing helium (He) as the carrier gas. The $\text{NH}_3\text{-TPD}$ process was monitored by an on line gas chromatograph equipped with a TCD detector. Typically 140 mg sample was pretreated at 600°C for 1 h in flowing He (25 ml/min), then cooled to 150°C and saturated with NH_3 . After that, the sample was purged with pure He for a certain period until a stable GC-baseline was attained. Subsequently $\text{NH}_3\text{-TPD}$ experiment was carried out in the range of $150\text{--}700^\circ\text{C}$ at a heating rate of $18.8^\circ\text{C}/\text{min}$.

^1H MAS NMR spectra were recorded on a Varian Infinityplus-400 spectrometer equipped with a 4 mm probe. Before the ^1H MAS NMR measurements, samples were dehydrated at 400°C under a pressure below 10^{-2} Pa for 20 h. Then ^1H MAS NMR spectra were collected at 399.9 MHz using single-pulse sequence with $\pi/4$ pulse, 4 s recycle delay with a spinning speed of 10 kHz. Chemical shifts were referenced to DSS. For the determination of quantitative results, all samples were weighed, and the spectra were calibrated by measuring a known amount of 1,1,1,3,3,3-hexafluoro-2-propanol performed in the same conditions [15]. The Dmfit software was used for deconvolution using fitted Gaussian-Lorentzian line shapes [16].

^{27}Al MAS NMR experiments were carried out on a Bruker AvanceIII-600 MHz spectrometer with a spinning rate of 15 kHz. Chemical shifts were referenced to $(\text{NH}_4)\text{Al}(\text{SO}_4)_2\cdot 12\text{H}_2\text{O}$ at 0.4 ppm as a secondary reference. The spectra were accumulated for 800 scans with a $\pi/12$ flip angle and a 2 s pulse delay.

Temperature-programmed reduction experiments under H_2 ($\text{H}_2\text{-TPR}$) were carried out in a conventional setup with a gas chromatography as the H_2 detector. The catalyst (80 mg) was loaded in a tubular quartz reactor, pretreated under flowing Ar of 20 ml/min at 550°C for 1 h, then cooled down to 100°C . Under flowing 10% H_2/Ar flow (20 ml/min), $\text{H}_2\text{-TPR}$ profiles were obtained in the range of $100\text{--}900^\circ\text{C}$ at a heating rate of $14^\circ\text{C}/\text{min}$.

3. Results and discussions

3.1. N_2 adsorption results

Table 1 lists the textural properties of $6\text{Mo}/\text{H}_n\text{Na}_{100-n}\text{M-30Al}$ catalysts. At low sodium exchange degree, a relatively small specific surface area of $105\text{ m}^2/\text{g}$ is observed for $6\text{Mo}/\text{H}_{38}\text{Na}_{62}\text{M-30Al}$. As the exchange degree increases, the specific surface areas of the catalysts gradually increase to 231, 276 and $281\text{ m}^2/\text{g}$ for $6\text{Mo}/\text{H}_{67}\text{Na}_{33}\text{M-30Al}$, $6\text{Mo}/\text{H}_{82}\text{Na}_{18}\text{M-30Al}$ and $6\text{Mo}/\text{H}_{100}\text{Na}_0\text{M-30Al}$, respectively. It is well known that mordenite has one-dimensional 12-MR channel ($0.74 \times 0.65\text{ nm}$) connected with 8-MR window side pockets (window size $0.34 \times 0.48\text{ nm}$). Previous reports indicated that sodium exchange first occurred selectively within the 12-MR channels, more sodium ions would locate in the 8-MR side pockets which may block the entrance of N_2 molecules during N_2 -adsorption process [17,18]. As the exchange degree increases, more and more sodium ions locating at the 8-MR window will be replaced by H^+ , which may increase the access of N_2 to side pockets, thus results in increased specific surface area of the catalysts. This proposition can be further testified by the fact that the increase of specific surface areas is mainly caused by the increase of micropore surface areas (Table 1). Moreover, the micropore surface area increases significantly at relatively low exchange degree ($6\text{Mo}/\text{H}_{38}\text{Na}_{62}\text{M-30Al}$ to $6\text{Mo}/\text{H}_{67}\text{Na}_{33}\text{M-30Al}$) and only minor increase occurs at high exchange degree ($6\text{Mo}/\text{H}_{82}\text{Na}_{18}\text{M-30Al}$ to $6\text{Mo}/\text{H}_{100}\text{Na}_0\text{M-30Al}$), which indicates that the sodium ions

Table 1
Textural properties and acidity information over 6Mo/H_nNa_{100-n}M-30Al catalysts.

Catalyst	BET surface area ^a (m ² /g)	Micropore area ^a (m ² /g)	Pore volume ^a (cm ³ /g)	Micropore volume ^a (cm ³ /g)	Brønsted acidity amount ^b (mmol/g)
6Mo/H ₃₈ Na ₆₂ M-30Al	105	46	0.1308	0.0208	–
6Mo/H ₆₇ Na ₃₃ M-30Al	231	150	0.1955	0.0694	0.142
6Mo/H ₈₂ Na ₁₈ M-30Al	276	178	0.2254	0.0828	0.175
6Mo/H ₁₀₀ Na ₀ M-30Al	281	187	0.2335	0.0871	0.221

^a Determined by N₂ adsorption isotherms.

^b Determined by quantitative analysis of ¹H MAS NMR spectra.

in 8-MR windows are the most difficult to be exchanged. The pore volume, especially the micropore volume, increases accordingly upon the exchange degree.

3.2. NH₃-TPD and ¹H MAS NMR results

Fig. 1 shows the NH₃-TPD profiles of the H_nNa_{100-n}M-30Al supports and 6Mo/H_nNa_{100-n}M-30Al catalysts. For H₃₈Na₆₂M-30Al support, only one NH₃ desorption peak at around 280 °C (nominated as *l*) is observed. No desorption peaks at high temperatures are found, which indicate that only weak acid sites present in the catalyst. After introduction of Mo species, the acid amount decreases from 0.671 to 0.446 mmol/g (Fig. 2). In the case of H₆₇Na₃₃M-30Al, a minor broad peak at around 500 °C (nominated as *h*) is observed in addition to the major peak at 280 °C (peak *l*). Mo loading leads to the peak intensity losses of both *l* and *h*. In order to get a more clear picture of the intensity changes of *l* and *h* peaks in the spectra, all the profiles are deconvoluted using Gaussian line and quantitative results are shown in Fig. 2. It is clear that upon increasing sodium exchange degree, the total acid amount of both the supports and catalysts increases. Moreover, the loss of acid amount by comparing the catalysts and the supports also increases upon the sodium exchange degree indicating that more acid sites participate in the interaction with Mo species. Combined with the N₂ adsorption results, it could be deduced that the dispersion of Mo species on 6Mo/H₁₀₀Na₀M-30Al is better than that of 6Mo/H₃₈Na₆₂M-30Al. As far as the peak intensity of *l* and *h* is concerned, an increasingly larger difference between *h*-support and *h*-catalyst could be observed, especially on 6Mo/H₁₀₀Na₀M-30Al catalyst.

High-resolution ¹H MAS NMR is a useful and direct method to characterize the Brønsted acid sites in the samples. Fig. 3 shows the ¹H MAS NMR spectra of 6Mo/H_nNa_{100-n}M-30Al catalysts. Due to the

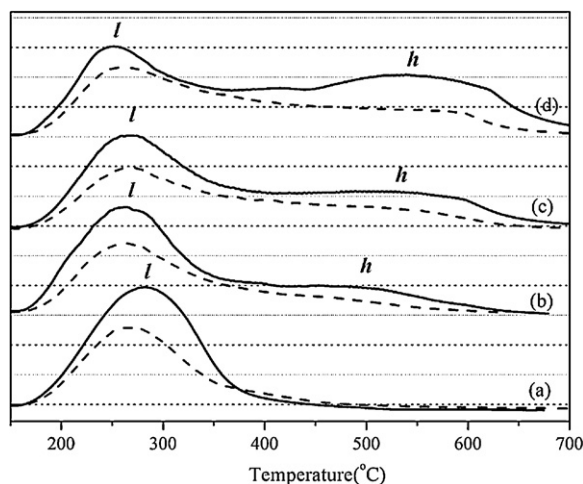


Fig. 1. NH₃-TPD profiles of H_nNa_{100-n}M-30Al supports in solid line and 6Mo/H_nNa_{100-n}M-30Al catalysts in dashed line: (a) 6Mo/H₃₈Na₆₂M-30Al (b) 6Mo/H₆₇Na₃₃M-30Al (c) 6Mo/H₈₂Na₁₈M-30Al (d) 6Mo/H₁₀₀Na₀M-30Al.

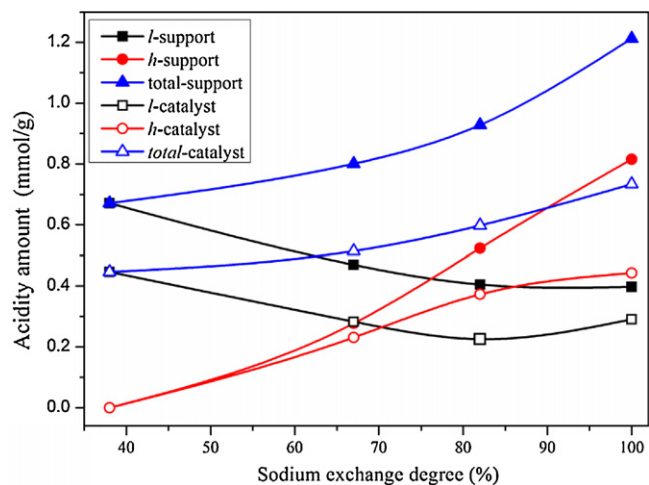


Fig. 2. Effects of sodium exchange level on the acidity amount of H_nNa_{100-n}M-30Al supports and 6Mo/H_nNa_{100-n}M-30Al catalysts determined from the quantitative analysis of NH₃-TPD profiles.

presence of alumina, the spectrum of 6Mo/H₁₀₀Na₀M-30Al is a little more complicated than that of H-mordenite zeolite [11]. As demonstrated in Fig. 3, the peak at 1.7 ppm is assigned to the silanol groups in H-mordenite zeolite; the signal at about 2.5 ppm may contain the contribution of non-framework Al–OH in H-mordenite zeolite and the acid hydroxyls in alumina [19]. The peak at 3.8 ppm is attributed to the bridging hydroxyl groups, i.e., Brønsted acid sites in H-mordenite. In the deconvoluted spectrum a broad line centered at ca. 5.9 ppm could be identified. It is ascribed to a second Brønsted acid site interacting electrostatically with the zeolite framework since it could be significantly suppressed after Al irradiation [19]. For the 6Mo/H₃₈Na₆₂M-30Al catalyst, the main resonance peak appears at 2.2 ppm which gradually shifts to low field position as the sodium exchange degree increases. A reasonable explanation

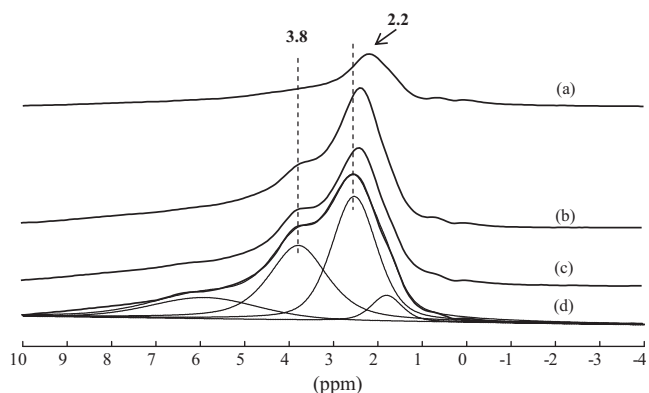


Fig. 3. ¹H MAS NMR spectra of 6Mo/H_nNa_{100-n}M-30Al catalysts: (a) 6Mo/H₃₈Na₆₂M-30Al (b) 6Mo/H₆₇Na₃₃M-30Al (c) 6Mo/H₈₂Na₁₈M-30Al (d) 6Mo/H₁₀₀Na₀M-30Al.

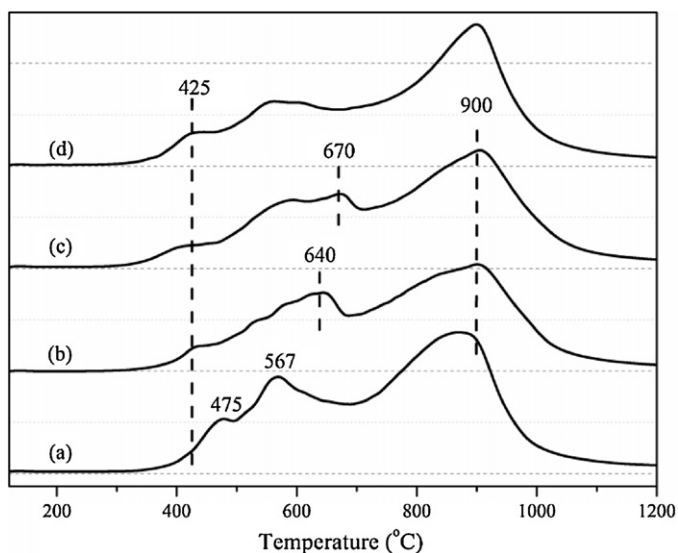


Fig. 4. H_2 -TPR profiles of $6Mo/H_nNa_{100-n}M$ -30Al catalysts: (a) $6Mo/H_{38}Na_{62}M$ -30Al (b) $6Mo/H_{67}Na_{33}M$ -30Al (c) $6Mo/H_{82}Na_{18}M$ -30Al (d) $6Mo/H_{100}Na_0M$ -30Al.

for this phenomenon is that the acidic hydroxyls from alumina (2.2 ppm) dominate the position of this peak when the sodium content is high. As sodium ion is gradually replaced by hydrogen, the peak intensity from non-framework Al–OH (2.4 ppm) in H-mordenite increases leading to a low field shift of the main peak. On $6Mo/H_{38}Na_{62}M$ -30Al sample, almost no bridge hydroxyl could be observed. This is in accordance with the NH_3 -TPD results as Brønsted hydroxyls are the main source of strong acid sites. Quantitative analysis of the spectra (Table 1) demonstrates that the concentration of Brønsted acid sites increases from 0.143 to 0.221 mmol/g when the sodium exchange degree changes from 67% to 100%.

3.3. H_2 -TPR and ^{27}Al MAS NMR results

From the above results, it is clear that changes of the sodium exchange degree in mordenite may result in variation of acid amount and distribution in the $H_nNa_{100-n}M$ -30Al support which may further influence the anchoring modes and location of Mo species on the support. Thus, H_2 -TPR experiments were performed to obtain more information about the redox behavior of $6Mo/H_nNa_{100-n}M$ -30Al catalysts. As shown in Fig. 4(a), three main reduction peaks locating at around 475, 570, and 900 °C could be differentiated on $6Mo/H_{38}Na_{62}M$ -30Al catalyst. With progressive exchange degree of sodium ions, the 475 °C peak shifts to high temperature. Meanwhile, a reduction peak appears at 425 °C. Simultaneously, the peak at 567 °C shifts to high temperature indicating the different distribution of Mo species on the support. The assignment to different reduction peaks is not straightforward due to the presence of different molybdenum species interacting with the surface to different extents. It is generally accepted that Mo species in tetrahedral state are difficult to reduce because of its strong interaction with the support, especially at low loadings. Octahedral and other higher polyhedral species are easy to be reduced. On basis of the earlier reports [20–22], reduction peak at 425 °C may be assigned to the first step reduction of $Mo^{6+} \rightarrow Mo^{4+}$ of the octahedral Mo species, especially for that on alumina. The high-temperature peak at around 900 °C may be related to the reduction of tetrahedral species as well as for the second step reduction of octahedral Mo species. The reduction peak at around 600 °C indicates the presence of polymeric Mo species linked with zeolite proposed by Solis et al. [22,23].

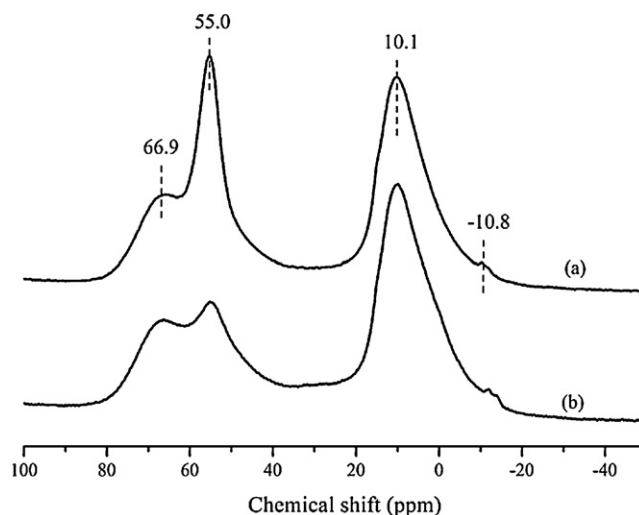


Fig. 5. ^{27}Al MAS NMR spectra of (a) $6Mo/H_{38}Na_{62}M$ -30Al and (b) $6Mo/H_{100}Na_0M$ -30Al.

From the N_2 adsorption results, it is clear that the micropore area of $6Mo/H_{38}Na_{62}M$ -30Al is low, possibly due to the blockage of sodium ions in the window of the side pockets. The location of sodium ions may further limit the entrance of Mo species into the channels. Thus, the dispersion of Mo species is poor on $6Mo/H_{38}Na_{62}M$ -30Al and most of the agglomerated Mo species are prone to locate at the outer surface of mordenite zeolite. When the sodium exchange level changes to 67%, the BET surface area increases to 231 m^2/g and more Brønsted acid sites are exposed for Mo anchoring which may lead to an improved dispersion of Mo species. Moreover, part of Mo species may immigrate into the channels of mordenite which leads to high temperature shift of the reduction peak. The peak at around 640 °C in Fig. 4(b) may be assigned to the reduction of polymeric Mo species locating inside the channels of mordenite zeolite. This is in well agreement with that of $Mo/ZSM-5-Al_2O_3$ catalysts with different Si/Al ratios of ZSM-5 [24]. Such trend is more obvious on $6Mo/H_{82}Na_{18}M$ -30Al. It is interesting that no such phenomenon is observed on $6Mo/H_{100}Na_0M$ -30Al catalyst. Compared with $6Mo/H_{82}Na_{18}M$ -30Al, the 670 °C peak shows a decrease in intensity in favor of an intensity enhancement of the peak at 900 °C. The increasing ratio of high-temperature reduction peak is related to the different distribution of Mo species on $H_{100}Na_0M$ -30Al support. It should be pointed out that the reduction peak at around 900 °C slightly shifts to high temperature upon sodium exchange degree as shown in Fig. 4. On basis of the discussion about reduction peak assignments, the reducibility of Mo species was closely related to its state and dispersion. The high-temperature shift in TPR profiles may be linked with the improved dispersion of Mo species on the support.

The varied distribution of Mo species on the support could be shown further by the ^{27}Al MAS NMR spectra. As shown in Fig. 5, two peaks in the tetrahedral region are observed. The signal at 55 ppm is assigned to framework tetrahedral aluminum in mordenite zeolite and the broad one centered at ca. 67 ppm comes from the four-coordinated aluminum in alumina. A marked peak intensity loss of framework aluminum (55 ppm) is observed on $6Mo/H_{100}Na_0M$ -30Al compared with that of $6Mo/H_{38}Na_{62}M$ -30Al which means more Mo species interact with the framework aluminum, i.e. Brønsted acid sites on the $H_{100}Na_0M$ -30Al support. In the case of $H_{38}Na_{62}M$ -30Al, Mo species tend to locate on alumina or aggregate on the surface of support due to the steric hindrance of zeolite channels from sodium ions. This is in accordance

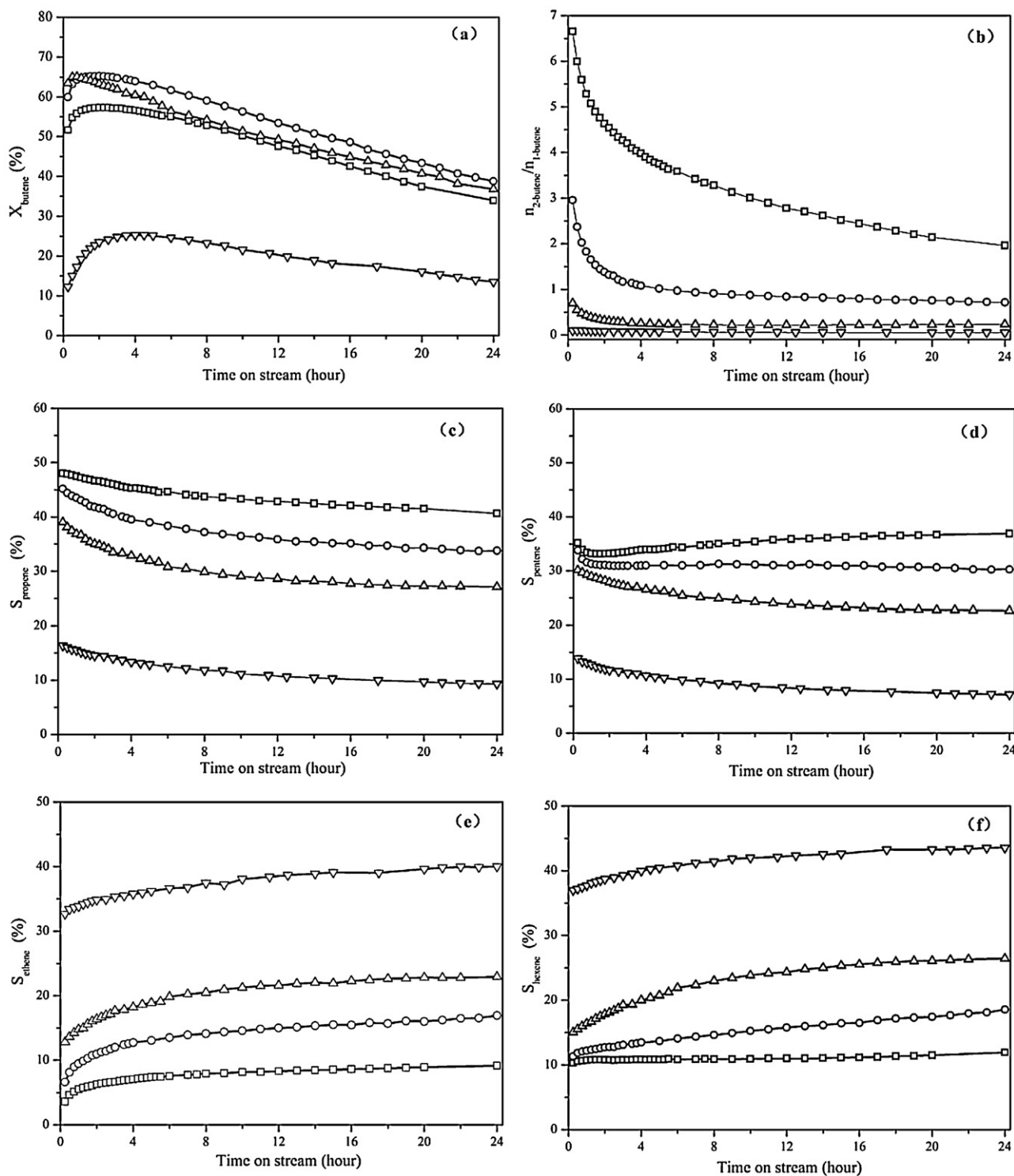


Fig. 6. Butene conversion and product selectivity over 6Mo/H_nNa_{100-n}M-30Al catalysts with different sodium exchange degrees in the support: (▽) 6Mo/H₃₈Na₆₂M-30Al (Δ) 6Mo/H₆₇Na₃₃M-30Al (○) 6Mo/H₈₂Na₁₈M-30Al (□) 6Mo/H₁₀₀Na₀M-30Al (reaction temperature: 150 °C, pressure: 0.1 MPa, WHSV of 1-butene: 2.0 h⁻¹).

with the H₂-TPR results. In the octahedral region, a broad signal centered at ca. 10 ppm is observed, which can be attributed to the six-coordinated aluminum in alumina. This signal is also overlapped with that from the non-framework Al in mordenite zeolite. Besides, a small peak appears at -11 ppm, corresponding to the nonhydrated forms of the aluminum molybdate phase [11,25,26]. Therefore, a chemical reaction between the Mo species and the support happens, which results in the formation of aluminum molybdate.

3.4. Metathesis activity of 6Mo/H_nNa_{100-n}M-30Al catalysts

1-Butene double-bond isomerization as well as metathesis may occur on 6Mo/H_nNa_{100-n}M-30Al catalysts. No skeletal isomerization product i.e. *iso*-butene is detected. A schematic representation of possible reaction pathways of 1-butene over 6Mo/H_nNa_{100-n}M-30Al catalysts is shown in Scheme 1. It is clear that propene, pentene, ethene and hexene are the main metathesis products. Propene may come from metathesis reaction of 1-butene and

Table 2
1-Butene metathesis and isomerization performance over 6Mo/H_nNa_{100-n}M-30Al catalysts (TOS: 4 h, temperature: 150 °C, pressure: 0.1 MPa, WHSV: 2.0 h⁻¹).

Catalyst	Y _{ethene} (%)	Y _{propene} (%)	Y _{pentene} (%)	Y _{hexene} (%)	Y _{2-butene} (%)	n _{1-butene} /n _{2-butene}
6Mo/H ₃₈ Na ₆₂ M-30Al	8.8	2.9	2.6	10.0	5.1	14.0
6Mo/H ₆₇ Na ₃₃ M-30Al	11.0	19.1	16.4	11.8	8.2	3.9
6Mo/H ₈₂ Na ₁₈ M-30Al	8.2	24.4	19.6	8.6	18.9	0.94
6Mo/H ₁₀₀ Na ₀ M-30Al	4.2	27.4	19.8	6.7	30.6	0.25

2-butene (Metathesis I) or metathesis of ethene and 2-butene (Metathesis III). Ethene and hexene are the products from 1-butene self-metathesis (Metathesis II).

Catalytic performances of 6Mo/H_nNa_{100-n}M-30Al catalysts in 1-butene metathesis reaction are shown in Fig. 6. For all the catalysts, their initial activity increases with time until the peak-point is attained. This is ascribed to the induction period during which metathesis active intermediates are generated in situ under olefin atmosphere. This is common to a number of catalysts, such as Mo/Al₂O₃ and Mo/SiO₂ catalysts used in propene metathesis [20,27,28]. It should be pointed out that a longer induction period is observed on 6Mo/H₃₈Na₆₂M-30Al which lasts about 4 h. That means the state of Mo species or the low acid density on 6Mo/H₃₈Na₆₂M-30Al is not beneficial for the rapid formation of active metathesis sites. As shown in Fig. 6(a), butene conversion is around 25% on 6Mo/H₃₈Na₆₂M-30Al, while 60% for the other three samples. A little higher conversion is observed on 6Mo/H₈₂Na₁₈M-30Al than that on 6Mo/H₁₀₀Na₀M-30Al. This may be linked with the isomerization activity of the catalysts as shown in Fig. 6(b). On 6Mo/H₁₀₀Na₀M-30Al, the initial molar ratio of 2-butene to 1-butene in the product is up to 6.6 and it remains above 2.0 after 24 h, much higher than that over other catalysts. High 2-butene concentration in the feed is not favorable for the metathesis of 1-butene and 2-butene, especially for 1-butene self-metathesis. Supposing that 2-butene self-metathesis happens during the process, the product could not be differentiated from the 2-butene isomers. Over 6Mo/H₈₂Na₁₈M-30Al catalyst, the molar ratio of 2-butene to 1-butene maintains around 1.0 during the total process, which is equal to the stoichiometry value of 2-butene and 1-butene metathesis reaction. On the other hand, the ratio is below 0.5 on 6Mo/H₆₇Na₃₃M-30Al sample. Such ratio is favorable for the 1-butene self-metathesis reaction. Poor isomerization activity is observed on 6Mo/H₈₂Na₁₈M-30Al due to its low acidity.

Propene selectivity is closely related to sodium exchange degree of the support. As shown in Fig. 6(c), the highest propene selectivity of about 47% is obtained on 6Mo/H₁₀₀Na₀M-30Al followed by 6Mo/H₈₂Na₁₈M-30Al, 6Mo/H₆₇Na₃₃M-30Al and 6Mo/H₃₈Na₆₂M-30Al with propene selectivity of about 40%, 30% and 15%, respectively, which following the same order of sodium contents. As shown in Scheme 1, propene could be obtained from Metathesis III besides Metathesis I. High 2-butene concentration in the feed is beneficial for Metathesis III which may well explain the trend of propene selectivity change. As far as the yield is concerned, 6Mo/H₁₀₀Na₀M-30Al gives the highest propene yield of about 27.4% as shown in Table 2. Due to the various routes for propene generation, it is rational that the selectivity for pentene is a little lower than that of propene on the same catalyst.

6Mo/H₃₈Na₆₂M-30Al exhibits the highest ethene and hexene selectivities which indicates that 1-butene self-metathesis dominates in the reaction network. In this case, Metathesis I is suppressed due to the low molar ratio of 2-butene to 1-butene. Although ethene is the dominant product on 6Mo/H₃₈Na₆₂M-30Al, its yield (8.8%) is lower than that of 6Mo/H₆₇Na₃₃M-30Al (11.0%). It could be concluded that the metathesis activity is closely linked with the catalyst acidity and location of the Mo species. Exposure of more acid sites in H₆₇Na₃₃M-30Al benefits the formation of dispersed Mo species which contributes to the high ethene yield on

6Mo/H₆₇Na₃₃M-30Al. On 6Mo/H₃₈Na₆₂M-30Al, hexene selectivity is a little higher than that of ethene. Such phenomenon is more obvious on 6Mo/H₁₀₀Na₀M-30Al as more ethene is consumed by Metathesis III.

Combining the characterization results with the catalytic performances, it is obvious that acid sites in mordenite zeolite of HM-30Al supports play two important roles in the 1-butene metathesis reaction. One is that the exposure degree of acid sites, especially strong acid sites may influence the location and state of Mo species on the support. As pointed out by Debecker and Handzlik et al., the existence of suitable number of Brønsted acid site is beneficial for the genesis of active metathesis centers [12,29]. Thus, high sodium exchange degree will contribute to the formation of metathesis active Mo species. The other role of acid site lies in its catalytic activity in 1-butene isomerization. Substantial amount of acid sites on the catalyst is required to guarantee the double bond isomerization which is the requisite step of the following objective metathesis reaction. To maximize propene yield, the rate of 1-butene double bond isomerization should match with that of the cross-metathesis of 1-butene and 2-butene. As shown in Table 2, 1-butene self-metathesis dominates on 6Mo/H₃₈Na₆₂M-30Al due to the limitation of 1-butene isomerization. On 6Mo/H₈₂Na₁₈M-30Al, the molar ratio of 2-butene to 1-butene amounts to 1.0 and the number of metathesis active site becomes the pivotal factor in determining the metathesis activity. Highest propene yield is obtained on 6Mo/H₁₀₀Na₀M-30Al due to its high acid density and well dispersion of Mo species.

4. Conclusions

Effect of sodium exchange degree on the performance of 6Mo/H_nNa_{100-n}M-30Al catalyst in 1-butene metathesis was investigated. It was found that the metathesis product distribution could be tuned through adjusting the surface acidity of the support which can be controlled by changing the sodium exchange degree of mordenite. Ethene (hexene) was the main product at high sodium content and propene gradually became the dominant product upon increasing sodium exchange degree. 6Mo/H₁₀₀Na₀M-30Al with highest sodium exchange degree exhibited the best metathesis performance, and high propene yield of 27.4% was obtained. Well dispersion of Mo species and high density of Brønsted acid site, as evidenced by H₂-TPR and ¹H MAS NMR results, benefit catalytic performance of 6Mo/HM-30Al.

Acknowledgments

We are grateful for the financial support of the National Natural Science Foundation of China (Grant No. 20903088 and 21006104).

References

- [1] X.X. Zhu, X.J. Li, S.J. Xie, S.L. Liu, G.L. Xu, W.J. Xin, S.J. Huang, L.Y. Xu, Catal. Surv. Asia 13 (2009) 1–8.
- [2] J.C. Mol, J. Mol. Catal. A: Chem. 213 (2004) 39–45.
- [3] K. Amakawa, S. Wrabetz, J. Kröhnert, G. Tzolova-Müller, R. Schlögl, A. Trunschke, J. Am. Chem. Soc. 134 (2012) 11462–11473.
- [4] D.P. Debecker, M. Stoyanova, F. Colbeau-Justin, U. Rodemerck, C. Boissière, E.M. Gaigneaux, C. Sanchez, Angew. Chem. Int. Ed. 51 (2012) 2129–2131.

- [5] L. Harmse, C. van Schalkwyk, E. van Steen, *Catal. Lett.* 137 (2010) 123–131.
- [6] Y. Wang, Q. Chen, W. Yang, Z. Xie, W. Xu, D. Huang, *Appl. Catal. A: Gen.* 250 (2003) 25–37.
- [7] D. Hua, S.L. Chen, G. Yuan, Y. Wang, Q. Zhao, X. Wang, B. Fu, *Micropor. Mesopor. Mater.* 143 (2011) 320–325.
- [8] S.J. Huang, H.J. Liu, L. Zhang, S.L. Liu, W.J. Xin, X.J. Li, S.J. Xie, L.Y. Xu, *Appl. Catal. A: Gen.* 404 (2011) 113–119.
- [9] D.Z. Zhang, X.J. Li, S.L. Liu, S.J. Huang, X.X. Zhu, F.C. Chen, S.J. Xie, L.Y. Xu, *Appl. Catal. A: Gen.* 439–440 (2012) 171–178.
- [10] J.N. Kondo, L. Shao, F. Wakabayashi, K. Domen, *J. Phys. Chem. B* 101 (1997) 9314–9320.
- [11] X.J. Li, W.P. Zhang, S.L. Liu, L.Y. Xu, X.W. Han, X.H. Bao, *J. Catal.* 250 (2007) 55–66.
- [12] D.P. Debecker, D. Hauwaert, M. Stoyanova, A. Barkschat, U. Rodemerck, E.M. Gaigneaux, *Appl. Catal. A: Gen.* 391 (2011) 78–85.
- [13] D.P. Debecker, B. Schimmoeller, M. Stoyanova, C. Poleunis, P. Bertrand, U. Rodemerck, E.M. Gaigneaux, *J. Catal.* 277 (2011) 154–163.
- [14] H.J. Liu, S.J. Huang, L. Zhang, S.L. Liu, W. Wang, W.J. Xin, S.J. Xie, L.Y. Xu, *Chin. J. Catal.* 29 (2008) 513–518.
- [15] M. Muller, G. Harvey, R. Prins, *Micropor. Mesopor. Mater.* 34 (2000) 281–290.
- [16] D. Massiot, F. Fayon, M. Capron, I. King, S. Le Calve, B. Alonso, J.O. Durand, B. Bujoli, Z.H. Gan, G. Hoatson, *Magn. Reson. Chem.* 40 (2002) 70–76.
- [17] V.D. Dominguez-Soria, P. Calaminici, A. Goursot, *J. Chem. Phys.* 127 (2007) 154710–154711.
- [18] J. Nagano, T. Eguchi, T. Asanuma, H. Masui, H. Nakayama, N. Nakamura, E.G. Derouane, *Micropor. Mesopor. Mater.* 33 (1999) 249–256.
- [19] H.M. Kao, C.Y. Yu, M.-C. Yeh, *Micropor. Mesopor. Mater.* 53 (2002) 1–12.
- [20] R. Thomas, J.A. Moulijn, *J. Mol. Catal.* 15 (1982) 157–172.
- [21] S. Rajagopal, H.J. Marini, J.A. Marzari, R. Miranda, *J. Catal.* 147 (1994) 417–428.
- [22] X.J. Li, W.P. Zhang, S.L. Liu, S.J. Xie, X.X. Zhu, X.H. Bao, L.Y. Xu, *J. Mol. Catal. A Chem.* 313 (2009) 38–43.
- [23] D. Solis, A.L. Agudo, J. Ramirez, T. Klimova, *Catal. Today* 116 (2006) 469–477.
- [24] D.Z. Zhang, X.J. Li, S.L. Liu, X.X. Zhu, W.J. Xin, S.J. Xie, P. Zeng, L.Y. Xu, *Chin. J. Catal.* 32 (2011) 1747–1754.
- [25] X.J. Li, W.P. Zhang, S.L. Liu, X.W. Han, L.Y. Xu, X.H. Bao, *J. Mol. Catal. A Chem.* 250 (2006) 94–99.
- [26] X.J. Li, W.P. Zhang, S.L. Liu, L.Y. Xu, X.W. Han, X.H. Bao, *J. Phys. Chem. C* 112 (2008) 5955–5960.
- [27] B. Zhang, N. Liu, Q. Lin, D. Jin, *J. Mol. Catal.* 65 (1991) 15–28.
- [28] R. Thomas, J.A. Moulijn, V.H.J. De Beer, J. Medema, *J. Mol. Catal.* 8 (1980) 161–174.
- [29] J. Handzlik, J. Ogonowski, J. Stoch, M. Mikolajczyk, P. Michorczyk, *Appl. Catal. A: Gen.* (2006) 213–219.